



Influence of Friction Stir Welding Parameters on Dissimilar Joints AA6061-T6 and AA5052-H32

S. Balamurugan¹ · K. Jayakumar¹ · K. Subbaiah¹

Received: 6 February 2021 / Accepted: 22 May 2021 / Published online: 12 June 2021
© King Fahd University of Petroleum & Minerals 2021

Abstract

In this present study, two dissimilar aluminum alloys of AA5052-H32 and AA6061-T6 were joined in butt joint configuration to examine the influence of process parameter on tensile strength and microstructural examination. Tool profiles such as square, cylinder, triangle with welding speeds like 30, 60, 80 mm/min and tool rotational speeds such as 800, 950, 1100 rpm were selected as process parameters for friction stir welding. Among the various tool profiles, square pin profile produced good pulsating action of 60 pulses and having max SV/DV ratio of 2.3 which helped to produce higher tensile strength. Microstructural examination on the nugget zone revealed that higher welding speed causes some cracks in the nugget zone due to insufficient stirring of the materials. Microhardness examination reveals that HAZ of both zones exhibited lower hardness on both sides. Nugget zone at centre was measured with increased hardness than BM of AA5052 and lower than AA6061. SEM fractography revealed that the specimens were failed in ductile mode and specimens failed at higher tensile strength observed with high ductility. Taguchi optimization technique has been implemented and the process parameters combination was optimized for higher tensile strength. The dissimilar joints fabricated at optimized process parameters produced maximum tensile strength of 181 MPa are as follows: Tool Profile—Square, Tool-Rotational Speed—1100 rpm and Welding speed—60 mm/min.

Keywords Dissimilar aluminium alloys · Optimization · FSW · AA5052 · AA6061

1 Introduction

Recently, modern industries are showing attention in joining of dissimilar aluminum alloys which produce an amalgamation of necessary properties of parent materials [1, 2]. The popular joining techniques for joining of dissimilar materials are conventional fusion welding process and solid state welding process. In conventional fusion welding process, selection of filler material for joining dissimilar materials is not easy. Also, there is a possibility of formation of brittle, complex and intermetallic compounds which results inferior weld joints [3]. On the other hand, solid state welding process also has some difficulties in joining dissimilar materials. But, suitable interlayer can prevent the intermetallic

compounds formation. So, solid state welding is good choice for dissimilar joining.

Among several solid state welding process, to weld the aluminium alloys (2xxx, 5xxx and 7xxx series) which are difficult to weld, the most prominent, well suited and efficient process is Friction Stir Welding (FSW) [4–6]. In this process, a rotating tool is used for creating friction when it plunges and moves along the faying sides of the joints. Moreover, FSW can attain peak temperature up to 95 per cent of the melting temperature (T_m) of the materials to be joined [7]. Some advantages of FSW are no filler metal is used, no toxic fumes are produced and skilled labour is not required to obtain good quality welds [8]. Due to the several advantages of this process, various industries such as ship building, automotive and aerospace are showing interest to implement this process [9, 10].

Various literatures may be seen regarding FSW in butt joint configuration, while many of them uniquely concentrates on similar and dissimilar joints of thin thickness alloys [11–13]. So, determination of effective process parameters on medium thickness (5 mm) dissimilar joints is necessary.

✉ S. Balamurugan
balarema1504@gmail.com

¹ Department of Mechanical Engineering, Sri Sivasubramaniya Nadar College of Engineering, Kalavakkam, Chennai 603110, Tamil Nadu, India



The preferable joint configuration in FSW welding is Butt joint, due to its easy setup and stress distribution. This joint configuration found in many industrial applications. One of the examples is resistance spot welding (RSW) is replaced by butt joints in automotive industry [14, 15]. Because overlapping of sheets is reduced in butt joint configuration which helps in reduction of weight. The future in industrial applications of FSW has been inspired by researchers and several studies have been done. Some instances are, Krasnowski et al. [16] examined the effect of tool geometry on FSW joints of Al 6082 alloy. They observed that, the conventional and Triflute tool produced good tensile performance on the joints produced by FSW. Cavaliere et al. [17] analysed the influence of FSW process parameters on metallurgical and mechanical on AA 6082 alloys by varying the welding speed and rotating speed is fixed. They reported that yield strength was increased in lower speeds and start decreased at higher speeds. Momeni et al. [18] analysed the influence of FSW process parameters at post weld heat treated conditions and reported that grain size is not affected by post weld heat treatment.

Rajkumar et al. [19] produced a similar joint of Al 5xxx series and examined the influence of weld speed and tool design on properties of mechanical. Kwon et al. [20] and Moshwan et al. [21] observed that similar joints of AA5052 produced a maximum yield strength at the tool speed of 1000 rpm. Mustafa et al. [22] successfully joined the AA6061 materials and Taguchi method was utilized for optimization of tool geometries on mechanical properties. Hong et al. [23] and Park et al. [24] reported that while welding of dissimilar aluminium alloys (6061 and 5052) the mixing of materials and joint strength were increased rapidly when keeping 5052 material in advancing side.

Most of these researchers examined the influence FSW parameters such as tool profile, welding speed and tool rotational speed on microstructural and mechanical properties of friction stir welded Al alloys and AZ31 alloys etc., To the best of our knowledge, no researchers optimized the combination of tempered and strain hardened conditions in FSW process. But, studies carried out using combination of all these FSW parameters on dissimilar welds of 5 mm thick plates AA6061-T6 and AA5052-H32 alloys are scarce. AA5052 (Al–Mg Alloy) has favourable characteristics such as good corrosion resistance and excellent weldability, due to this,

these material broadly used in automotive applications [25]. Also, AA5052 can be strengthened by dislocation, solid solution and grain boundary strengthening because it is a solid solution alloy. Another material widely used in automotive structural applications is AA6061 (Aluminium Alloy of Al–Si–Mg) because of its attractive amalgamation of good strength at low cost. Also, AA6061 is generally strengthened by precipitates because it is a heat treatable alloy. Joining the above alloys is most preferable because these dissimilar joints can have the combinations of superior corrosion resistance (AA5052) and the adequate strength (AA6061). So, the objective of this work is to examine the influence of tool profile, welding speed and rotational speed on mechanical and metallurgical properties in FSW dissimilar welds of AA6061-T6 and AA5052-H32 alloys. The reason for choosing dissimilar Aluminium alloy materials AA5052-H32 and AA6061-T6 as a part of study is due to their frequent application in automobile panels and aircraft structures.

2 Characterization and Testing Methods

2.1 Materials and Methods

The materials selected for this research are AA5052-H32 & AA6061-T6 with 5 mm thickness. The chemical composition and physical, mechanical properties of these materials are shown in Tables 1 and 2 respectively. The workpieces are cut into the dimensions of 100 mm × 10 mm × 5 mm Before welding the selected aluminum alloys were machined using milling equipment in the length–thickness plane (Transverse Long Section Plane). This could be helped to have a good contact at the mating surfaces at butt joint configuration. As the next step, these alloys were cleaned prior to welding using acetone which was keep the alloys free from

Table 2 Physical and mechanical properties of base materials

Material	Density (g/cm ³)	Melting point (°C)	Vickers hardness (HV ₁)	Tensile strength (MPa)
AA5052-H32	2.68	605	68	155
AA6061-T6	2.70	650	107	225

Table 1 Chemical composition of AA5052—H32 & AA6061—T6 aluminium alloys (Wt.%)

Alloy	Si	Mn	Mg	Zn	Cu	Cr	Fe	Al
AA5052-H32	0.21	0.1	2.4	0.1	0.1	0.32	0.39	Balance
AA6061-T6	0.57	0.09	0.9	0.20	0.18	0.01	0.33	Balance

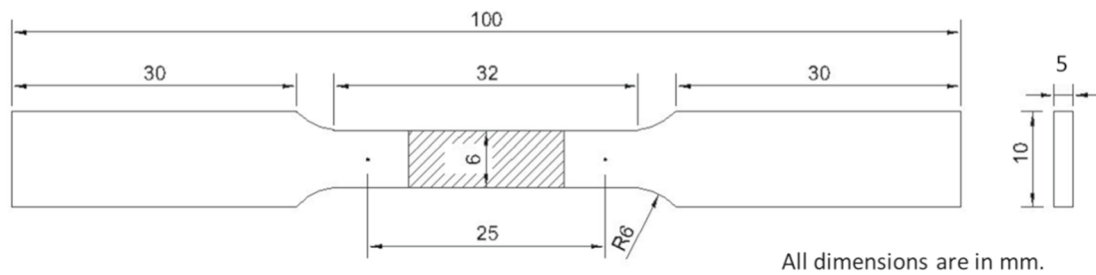


Fig. 1 Schematic diagram of tensile test sample

dirt, fine particles and organic material. After the welding has been completed the samples were prepared for the tensile test as depicts in Fig. 1.

2.2 Selection of Tool Profiles and Welding Parameters

The selected tool profiles for this study are square, cylindrical and triangular in shape. The shoulder height and diameter of the tool are 4.7 mm and 15 mm respectively. All the selected three tool pins have common dimension of 5 mm in diameter, side and base for cylinder, square and triangle respectively. The present research was conducted on the basis of different pin profiles with one of the dimensions as constant. The study didn't consider constant area and analysed the effect of tool pin profiles since the constant area may have less effect. The authors Balasubramanian et al. [26] and Shanmuga Sundaram and Murugan [27] were also used different profile pin profiles (square, triangle, circle, hexagon, etc.) without constant area. The actual profile and 2D diagram of the tool pins are depicted in Fig. 2a, b respectively. The tools used to join the selected dissimilar alloys are made up of H13 tool steel. The shape of the tool is casted, and heat treated. After heat treatment, for next three days tool was exposed to oil bath which was helped the tool to gain more strength. The FSW process parameters selected for this research are tool pin profile, welding speed in mm/min and tool rotation speed in rpm. Each parameter has three levels and listed in Table 3.

2.3 Experimental Setup

FSW joints were implemented on dissimilar aluminium alloys using an indigenously designed and developed machine shown in Fig. 3. The specifications of this machine are as follows: Max Load Capacity = 300 kN, Maximum spindle speed = 3000 rpm, Motor Capacity = 1.5 HP. Specimens were rigidly fixed using the fixture for perfect positioning and clamping the work pieces rigidly. For all welding trials AA5052 kept in advancing side. Experiments were

well planned and conducted as per the experimental design matrix mentioned in Table 4. Also, three samples were prepared for each trial. In which, two samples were utilized for obtaining tensile strength and the average values were given in Table 4. And, one sample is utilized for metallographic examination.

2.4 Design of Experiments

In this research work, to examine the effect of FSW process parameters on weld strength, three parameters have been chosen and each parameter has three levels as mentioned in Table 3. For that purpose, Taguchi's L27 orthogonal array was chosen, and the experimental runs with results are displayed in Table 4.

2.5 Metallographic Characterization

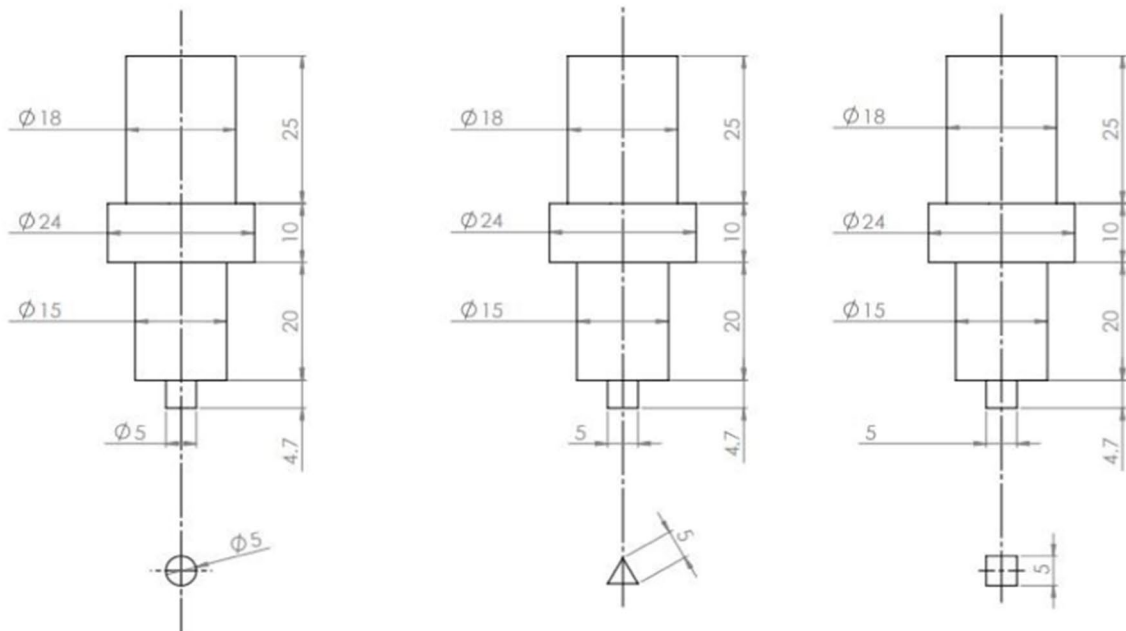
After the welding process completed, specimens were cut along the weld for obtaining the cross section of the FSW dissimilar joints. The obtained samples of the cross sections were ground and polished adhere with standard metallographic procedures. Further, to observe the clear microstructure Keller's reagent was applied as etchant. Keller's reagent is a solution of 5 ml HNO₃, 2 ml HF, 190 ml, 3 ml HCl and H₂O. Optical microscope was used to observe the microstructures of cross sectioned samples. To study the elemental mapping of the welded surface the samples were subjected to XRD (X-Ray Diffraction) analysis and SEM (Scanning Electron Microscopy).

2.6 Mechanical Characterization

Vickers microhardness and tensile test examinations were carried for mechanical characterization. Wilson Wolpert—Germany make micro Vickers hardness tester was used for hardness test by applying a dwell time of 10 s and load of 0.1 kgf with 0.005 m intervals. For tensile test, samples were prepared in dog-bone shape with dimensions of 25 mm gauge length and 6 mm width as per the standard of



(a)



(b)

Fig. 2 a Actual tool pin profiles. b 2D diagram of the tool pin profiles

ASTM-E8 (Fig. 1). Further, the samples were subjected to tensile testing at ambient temperature using uniaxial quasi static machine integrated with extensometer having a cross-head movement of 2 mm/min. Consequently, failed tensile

samples were subjected to SEM analysis to study the fracture surface. To avoid natural aging influence on mechanical characteristics of welded joints, after welding, the mechanical testing was completed in two days.

Table 3 Range of FSW parameters

Parameters	Level 1	Level 2	Level 3
Welding speed (mm/min)	30	60	80
Rotational speed (rpm)	800	950	1100
Tool profile	Square	Triangle	Cylinder



Fig. 3 FSW process machine

2.7 Taguchi Analysis

To examine the influence of parameters on FSW process many technologists use the procedure that changing the any single parameter and maintaining the remaining parameters constant. Such an investigational approach utilizes more sources and it is a time consuming process [28]. Alternatively, a novel method was introduced by Taguchi which was based on Orthogonal Array (OA) experiments. This method helps to achieve much reduced variance with optimum control parameters settings in minimal trials. In this optimization technique OA and Signal/Noise (S/N) ratio are acting as objective functions of desired output; useful in data analysis and optimum results prediction [29, 30]. Also, among the several techniques, Taguchi technique is the simplest and robust technique which can utilize less time and sources that can be recommended to optimize the process parameters for produce good quality products [31, 32].

Table 4 Experimental design matrix (L27)

Trial number	Tool pin profile	Welding speed (mm/min)	Rotational speed (rpm)	Tensile strength(MPa)
1	1	1	1	165.84
2	1	1	2	167.21
3	1	1	3	170.88
4	1	2	1	174.27
5	1	2	2	175.92
6	1	2	3	181.52
7	1	3	1	164.00
8	1	3	2	164.78
9	1	3	3	165.29
10	2	1	1	148.01
11	2	1	2	148.61
12	2	1	3	157.00
13	2	2	1	159.37
14	2	2	2	162.10
15	2	2	3	162.18
16	2	3	1	145.90
17	2	3	2	145.94
18	2	3	3	148.01
19	3	1	1	133.85
20	3	1	2	134.48
21	3	1	3	138.00
22	3	2	1	138.45
23	3	2	2	140.00
24	3	2	3	142.03
25	3	3	1	114.00
26	3	3	2	124.00
27	3	3	3	133.77

Therefore, in this research work, Taguchi optimization technique was implemented to optimize the FSW process parameters using L27 orthogonal array, that is 3 parameters has been chosen and each parameter has three factors as mentioned in Table 3. Initially, tensile strength for all the trials was averaged and the obtained value is known as overall mean. As the next step each trial value was squared, and all the squared values were added. The value obtained is known as SS_T (Grand-Total Sum-of-Squares). Sum-of-squares due-to-mean $(SS)_M$ was calculated as the product of number of trials conducted and the squared value of overall mean. The difference of $(SS)_T$ and $(SS)_M$ is known as total-sum-of-squares. Degree of freedom (DOF) is calculated as the difference of total sum of squares and sum of DOF for various factors. The ratio of sum-of-squares to the total-sum-of-squares gives percentage of contribution [29, 33].

3 Results and Discussion

3.1 Influence of Process Parameters on Tensile Strength

From Fig. 4 it can be seen that, each individual selected parameter have produced different effects on tensile strength. Figure 4a confirms that the tensile strength is increasing in the given order of changing the tool profile from cylinder, triangle and square. Among the three pin profiles, welded joints produced by square pin profile shows greater performance on tensile strength. This is due to the square tool having higher pulsating actions (60 pulses) with a ratio of Static Volume to Dynamic Volume of 1.56 which results in sweep or stirrer high amount of materials from plasticized zone. The joints produced by using triangular pin exhibits low tensile strength compared to joints fabricated by square pin. This is due to triangular pin having pulsating action of 45 pulses and exhibits high DV/SV ratio of 2.3. The joints produced by cylindrical pin are experiencing very low tensile strength because very low DV/SV ratio (1.0) and experiencing no pulsating actions.

Figure 4b depicts the influence of tool rotational speed on tensile strength. It is noticed that increasing tool rotational speed effectively increasing the tensile strength. This is because; increase in tool rotational speed allows the material to stirrer properly in the nugget zone. Figure 4c displays influence of welding speed on tensile strength. The tensile strength is increasing to certain level after that is fall suddenly. It is due to the fact that welding speed or travel speed

increases the time for stirring the materials will be reduced which results inferior joints. All specimens were failed in the nugget zone notably in AA5052 side.

3.2 Influence of Process Parameters on Microscopic Examination

Nugget zone is identified as stirred zone, also known as dynamically recrystallized zone which can ascertain by greater plastic deformation. All the NZ's (Fig. 5A–C) are observed with fine equiaxed grains but in various sizes. This difference in grain sizes are due to heat generation and rate of cooling during the FSW process. Generally, the following two mechanisms (1) CDR—Continuous dynamic recrystallization (2) DDR—Discontinuous dynamic recrystallization are the main reason for grains development in FSW process [34, 35]. In FSW, the contact between the tool and workpiece produces heat and causes excessive deformation of specimens. The former carries the probability for rearrangement of dislocations and the latter effects the increase in dislocation density. Thus, CDR and DDR occurs and microstructure of NZ observed with fine equiaxed grains [36]. It is evident from Fig. 4a, raising the travel speed from 30 mm/min to 60 mm/min which result an appropriate volume of materials are processed (Fig. 5A-(a) and B-(b)). But, when welding speed is increasing further to 80 mm/min, higher welding speeds causes poor stirring of materials which produced some cracks in the weld nugget. These cracks can reduce the tensile strength of the welded joint. This is because raise in welding speed reduce the time for

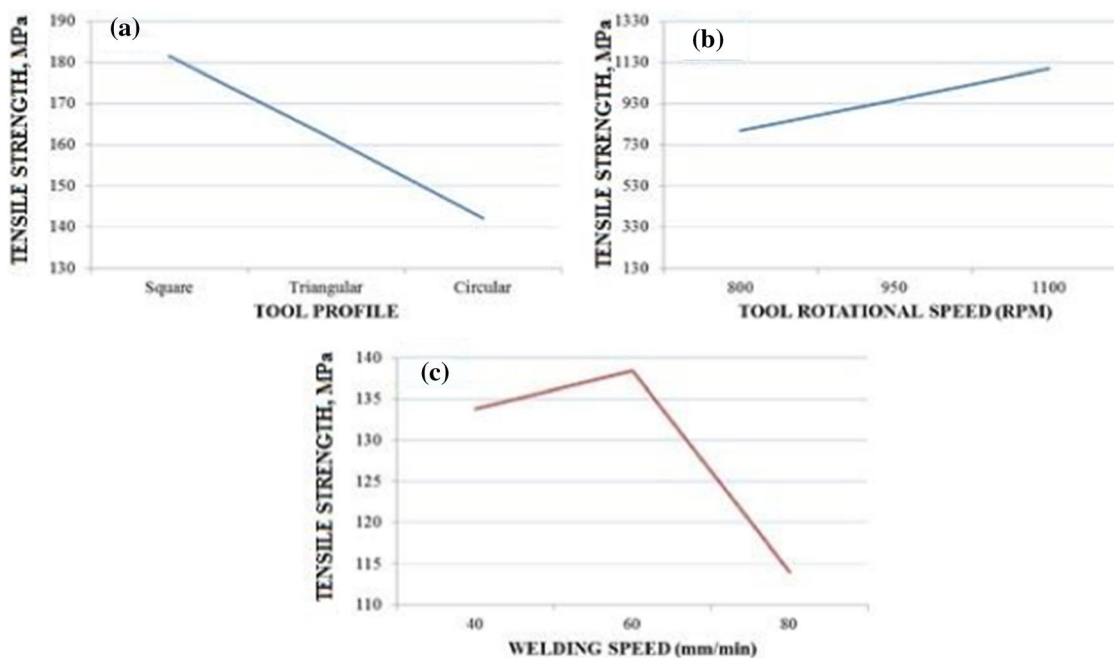


Fig. 4 Effects of process parameters on tensile strength



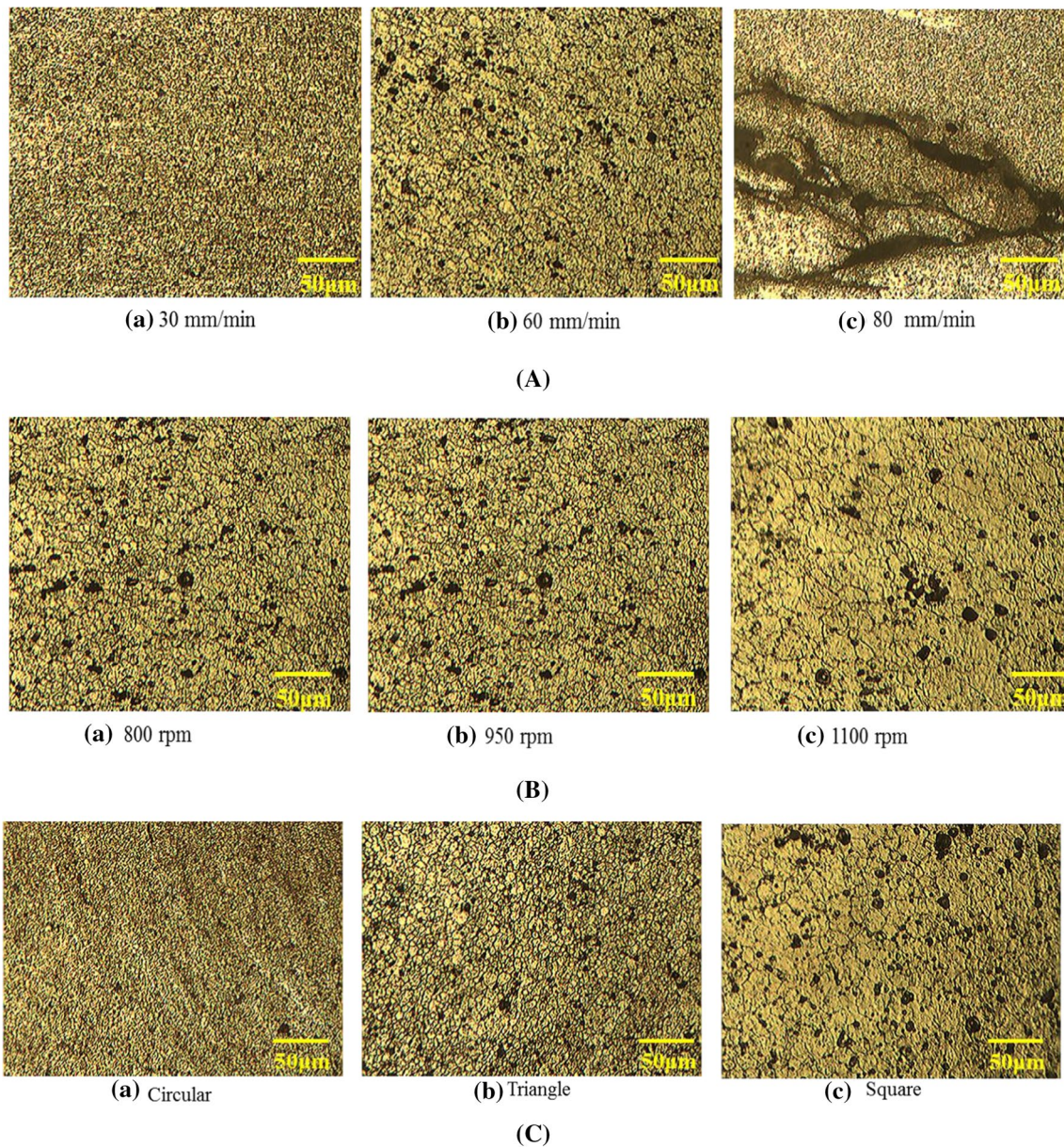


Fig. 5 **A** Microscopic images for nugget zone on various welding speeds when constantly maintaining tool profile and tool rotational speed as cylindrical and 800 rpm. **B** Microscopic images for various tool rotational speeds when constantly maintaining tool profile and

welding speed as triangle and 30 mm/min. **C** Microscopic images for tool profiles when constantly maintaining tool rotational speed and welding speed as 1100 rpm and 60 mm/min

stirring the materials. So, it is advised to reduce the welding speed. Effect of tool rotation speed on NZ microstructure is depicted on Fig. 4B-(a–c).

As compared to Fig. 5B-(a, b), Fig. 5B-(c) shows the grains in the NZ are highly refined with equiaxed grains [19, 37]. This is because there is a positive relationship between tool rotation speed and heat generation. Therefore, increasing tool rotation speed can effect with more

temperature. Sato et al. [36] agreed that the following Equation-1 can give a relationship between grain size and temperature. Thus the Eq. 1 proves that the increase in temperature causes increases in grain size [38].

$$d = \ln \frac{At}{2} - \frac{Q}{2RT} \tag{1}$$

where d is grain size, A is constant, t —time, T —temperature, R —gas constant and Q —activation energy.

Also, another fact is if welding time decreases or tool travel speed increases the contact time between tool and work pieces is reduced results lower heat generation causes reduction of grain growth (Fig. 5A-(c)).

Cylindrical pin produced very low tensile strength due to inadequate material stirrings as compared with other two pin profiles. Because, triangular and square pin profiles are connected with eccentricity which allows incompressible alloys or material to cover over the profile of the pin. Due to the rotating pin profile exhibits eccentricity, it can be linked with dynamic orbit. In FSW process, one of the fragments is dynamic orbit [39]. The flow of path of the plasticized material around the tool from leading edge to trailing edge can be related with a ratio of static volume (SV) to the dynamic volume (DV) [40]. This ratio for cylindrical, triangle and square tool pin profiles are equivalent to 1.0, 2.3 and 1.56 respectively [40]. As compared to Fig. 4C-(a, b), Fig. 4C-(c) shows grains in the NZ are highly refined with equiaxed recrystallized grains and precipitates scattered in a finer matrix which is the possible reason to produce higher tensile strength. This is due to the fact that square pin profile exhibits higher number of pulsating action and adequate SV/DV ratio as discussed in Sect. 3.1 [19, 37]. Another fact is that, among the three various pin profiles, square pin profile can easily affect the generation of heat [41, 42].

The trials which produced maximum, medium and least tensile strengths were selected for microscopic examination on HAZ. The selected trials are in the following

order: pin profile, Welding speed and rotational speed such as (1 Square pin, 60 mm/min and 1100 rpm (Trial 6—181.52 MPa) (2) Triangular pin, 30 mm/min and 950 rpm (Trial 11—148.61 MPa) (3) cylindrical pin, 80 mm/min and 800 rpm (Trial 25—114 MPa).

Figure 6a–c shows optical microscopic images of HAZ and (Thermo Mechanical Affected Zone) TMAZ for different trials. It is noticed that HAZ is separated by a distinct boundary. From Fig. 6a, it is evident that HAZ is affected by thermal cycle largely at trial 6 and no plastic deformation has been observed. But, TMAZ has been noticed by Grain growth due to the presence of plastic deformation. It is due to the fact that, square pin profile produces more heat during the welding process as compared to other pin profiles.

3.3 Microhardness and XRD Examination

The microhardness test has been conducted for all the trials and an average value at each point is shown in Fig. 7. During FSW process refinement of grain size is occurred due to large amount of heat generation which shows difference in hardness values throughout the nugget. The HAZ is the junction of tool shoulder, the lowest hardness values were observed on both sides of the materials. Dissolution of precipitates and severe coarsening due to thermal effect are the reasons for lower hardness in HAZ of AA6061 [43]. While, reason for lower hardness in AA5052 HAZ is being annealing phenomena [24]. Moreover, average hardness value of the NZ is higher at the center of the nugget. This can be explained that, the refined and equiaxed grains in center of

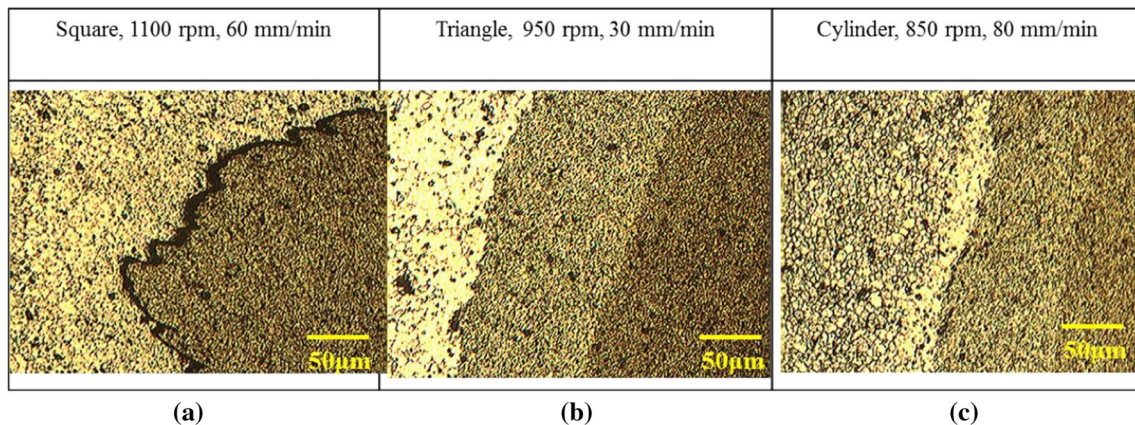


Fig. 6 a–c Optical Microscopic Images of HAZ and TMAZ for different trials

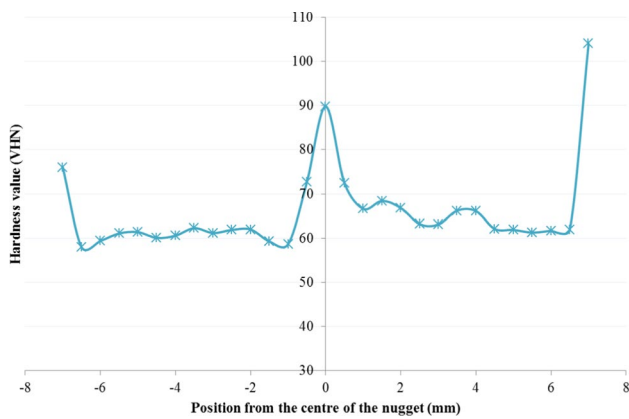


Fig. 7 Microhardness graph

the nugget causes increased in hardness. This is explained further in metallographic section. Another fact is that, during FSW process, the precipitation of second phase of Al_3Mg_2 and Mg_2Si from solid solution of Al-matrix can be seen in the Centre of the nugget and it is confirmed by XRD analysis (Fig. 8).

Therefore, the FSW joining of dissimilar AA5052-H32 and AA6061-T6 alloy has produced highest tensile strength of 181.52 MPa for the square pin profile. This value is 17% higher than the base metal of AA5052-H32 and 19% lower than the AA6061-T6.

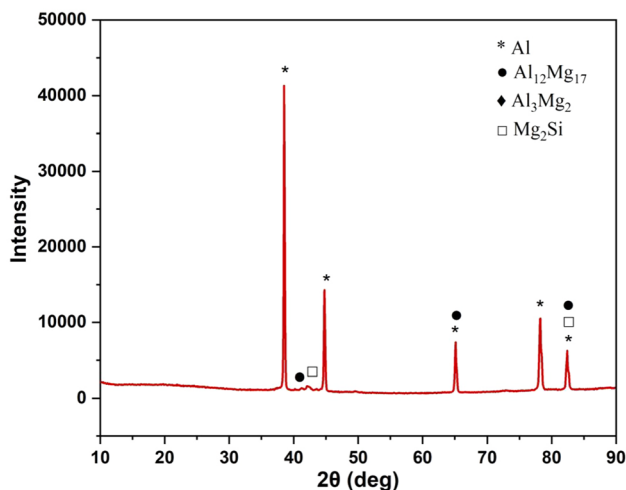


Fig. 8 XRD pattern of dissimilar aluminium alloys joint

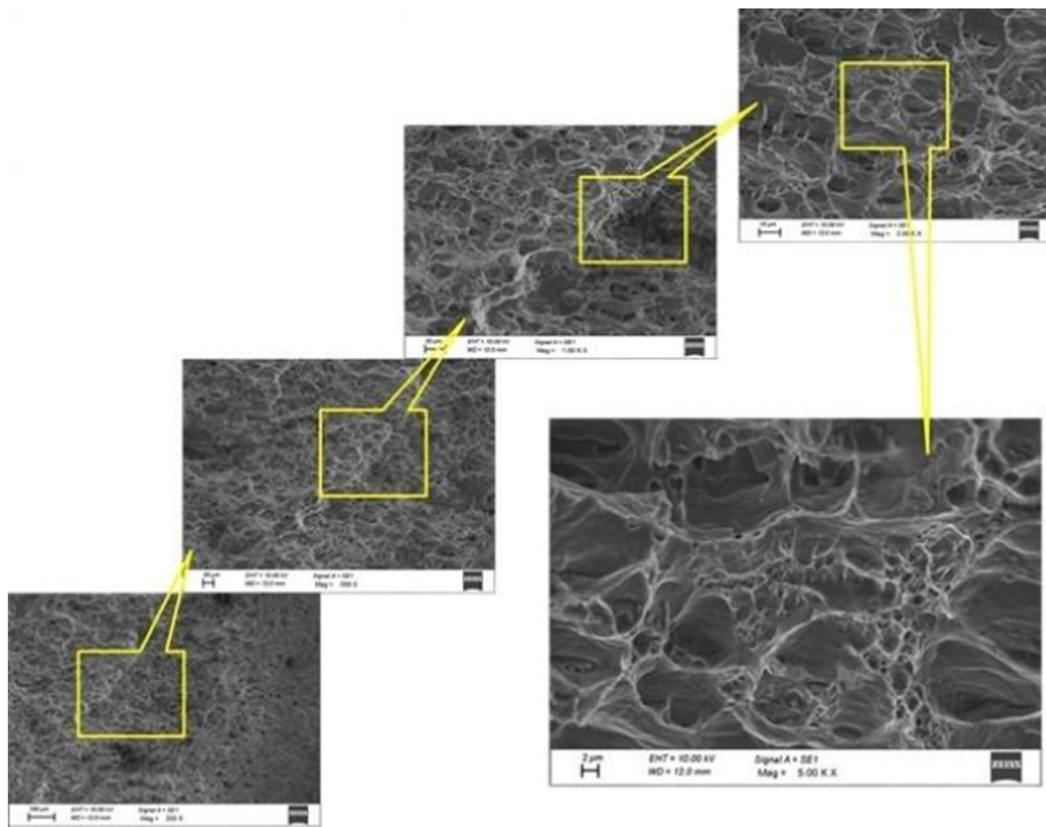
3.4 Fractography Examination

The samples failed at lower and higher tensile strength were considered for fractography analysis. Failed samples surface was subjected to SEM examination for understanding the mode of failure. Figure 9a, b shows SEM image of fractured surfaces which failed in lower and higher tensile strength respectively. The both specimens are observed with ductile fracture and it can be confirmed by presence of dimples in Fig. 9a, b. It is evident from the SEM fracture images of specimen failed at high tensile strength shows more intense ductility as compared to specimen failed at low tensile strength. This can be explained with Fig. 9a which is observed with tiny shallow dimples and whereas Fig. 9b noticed with some large dimples caused by coalescence of micro dimples which results high plastic deformation.

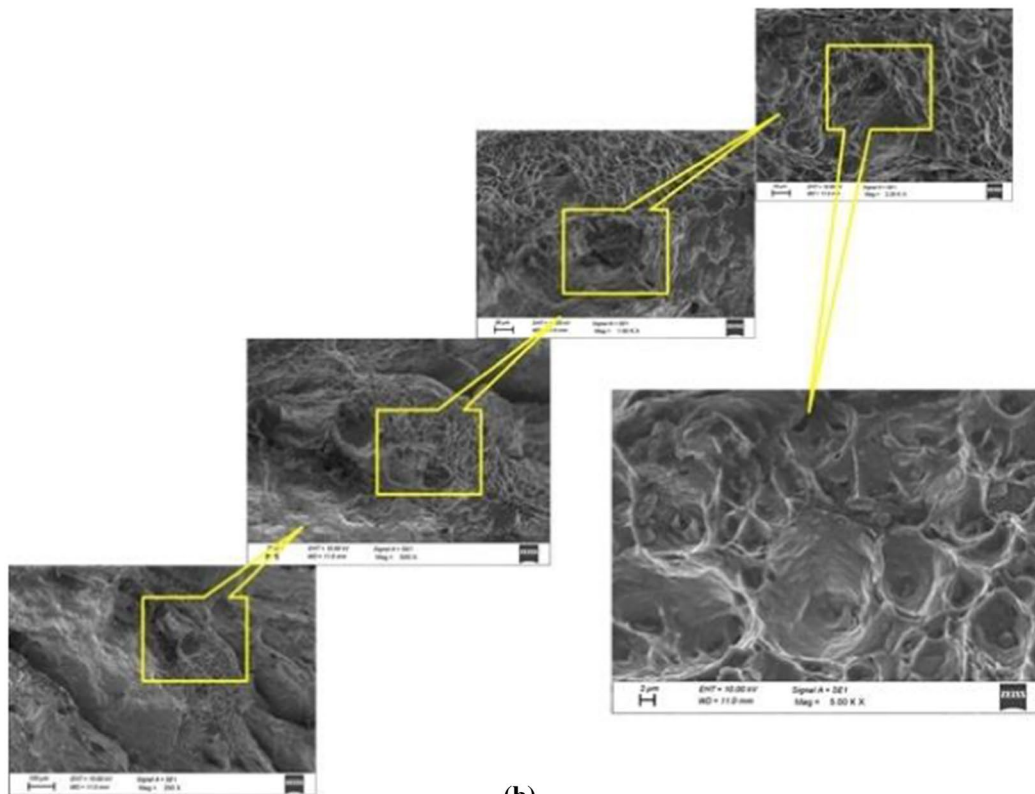
3.5 Taguchi Analysis

To perform this analysis LB_H (Larger the better) quality characteristic was considered because tensile strength is an implicit property of welded joints which should be always as high as possible. Figure 10a, b depicts the main-effect plot (MEP) for means and SN ratios which provides the facts about the effect of selected FSW parameters on tensile-strength. From the system response, the main effect plots can give a basic idea about the relative importance of the selected parameters. In the MEP, for a particular parameter a graph line is showing horizontal, then it is understood that there is no significant effect. In contrast, for any parameter a graph line is showing highest inclination in the MEP, then it is understood that the parameter is having most significant effect. From the given Fig. 10a, b it can be seen that tool pin profile has most significant effect on tensile strength. Also, from the given figures it is also came to know that all parameters having some influence on tensile strength.

Generally, high SN ratio results higher tensile strength of the welded joints. Hence, Figure 10 gives information about the combination of optimal parameters which provides higher tensile-strength and the optimal parameter combination is displayed in Table 5. Stress strain curve and weld profile for the optimal parameter’s combination (trial 6) is shown in Fig. 11a, b respectively. Also, it is noticed from Fig. 11c that, fracture occurred in AA6061 side due to recrystallization of microstructure.



(a)



(b)

Fig. 9 **a** Fractured surface SEM images for the specimen failed at low tensile strength. **b** Fractured surface SEM images for the specimen failed at high tensile strength

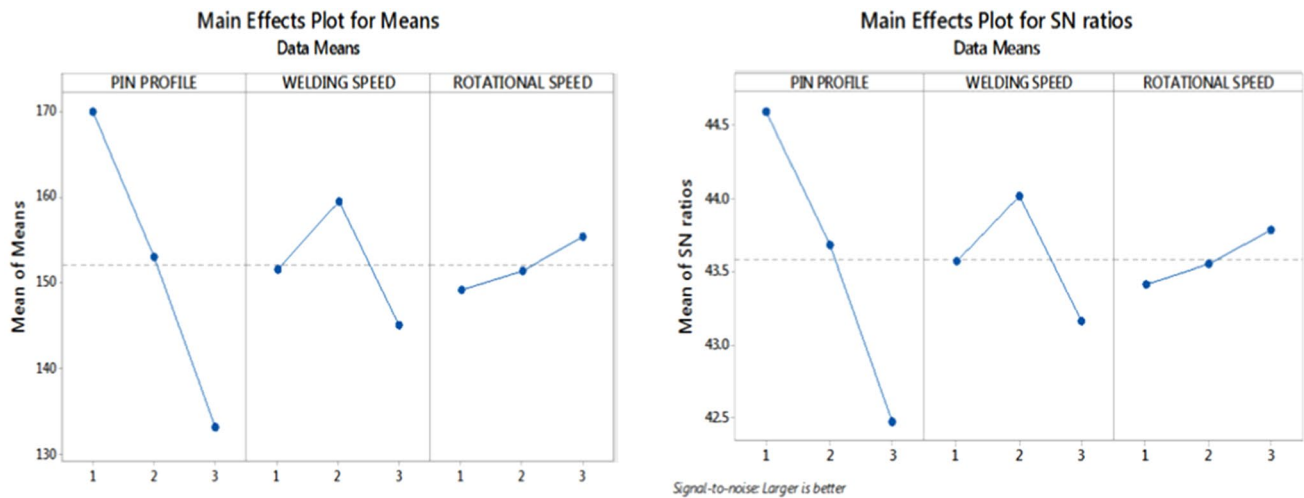


Fig. 10 a Main effects plot for means, b main effects plot for SN ratios

Table 5 Optimal parameter for higher tensile strength

Welding speed (mm/min)	Rotational speed (rpm)	Tool profile
60	1100	Square

According to the results of ANOVA given in Table 6, it is evident that pin profile is the dominant and the most effective parameter and rotational speed has second effective parameter and welding speed is the least effective. It is due to the fact that shape of the pin profile straightly affects the flow of material and shearing action of materials to be welded [44].

4 Conclusions

The dissimilar aluminium alloys of AA6061-T6 & AA5052 – H32 were joined using FSW process and results are given below.

1. The following optimal process parameters have produced good tensile strength of 181.52 MPa during FSW of AA5052-H32 and AA6061-T6. Tool profile: Square,

Tool Rotational Speed: 1100 rpm and Welding speed: 60 mm/min.

2. Tensile strength is increased with changing the tool profile in the following order. Cylindrical, Triangular and Square. Cylindrical tool profile showed very low tensile strength due to experiencing no pulsation action and low SV/DV (1.0) ratio. Square tool profile produced higher tensile strength due to high pulsating action of 60.
3. Microstructural examinations revealed that square pin profile showed finer and equiaxed grains as compared to other pin profiles. Also, at higher welding speed some cracks were observed in the microstructure due to insufficient stirring of materials.
4. Microhardness values for HAZ’s of both sides are observed with lower hardness due to the following reasons (1) dissolution of precipitates and severe coarsening in AA6061 side and (2) annealing phenomena in AA5052 side.
5. Fractography examination confirmed that specimens were failed at ductile mode of failure. The specimens failed at higher tensile strength observed with large dimples which was caused by coalescence of micro dimples that result high plastic deformation.

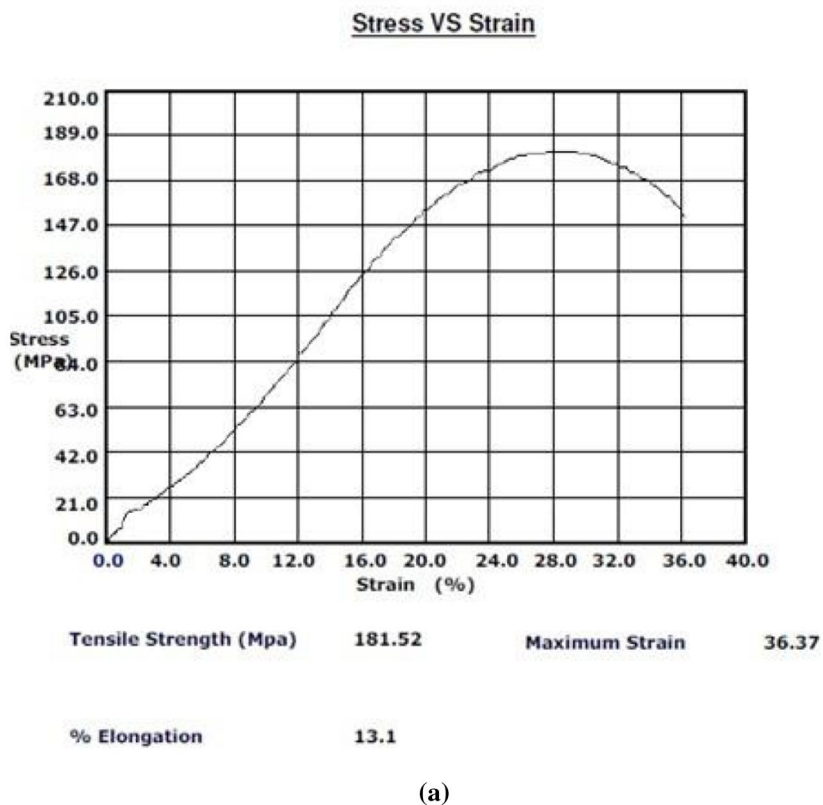


Fig. 11 a Stress–strain curve for optimal parameter combinations (trial 6). b Weld profile for the optimal parameter combinations. c Fractured specimen for the optimal parameter combinations

Table 6 ANOVA for tensile strength

Parameters	DOF	Sum of squares	Mean	Variance	Percentage of contribution
Pin profile	2	6104	3051.99	300.31	82.17
Rotational speed	2	944.6	472.28	46.47	12.7
Welding speed	2	172.9	86.45	8.51	2.3
Residual error	20	203.3	10.16		
Total	26	7427.7			

Author contributions SB—Conceptualization, investigation, writing—review & editing, KJ—supervision, technical review & validation, KS—resources, supervision, & validation.

Funding This work is not funded by any agency.

Declarations

Conflict of interest The authors declare that they have no known competing financial interests or personal relationships that could have appeared to influence the work reported in this paper.

References

- Chen, Y.; Ding, H.; Cai, Z.; Zhao, J.; Li, J.: Microstructural and mechanical characterization of a dissimilar friction stir-welded AA5083-AA7B04 Butt Joint. *J. Mater. Eng. Perform.* **26**, 530–539 (2017)
- Singh, V.P.; Patel, S.K.; Ranjan, A.; Kuriachen, B.: Recent research progress in solid state friction-stir welding of aluminium-magnesium alloys: a critical review. *J. Mater. Res. Technol.* **9**(3), 6217–6256 (2020)
- Goel, P.; Khan, N.Z.; Khan, Z.A.; Ahmar, A.; Gangil, N.; Abidi, M.H.; Siddiquee, A.N.: Investigation on material mixing during FSW of AA7475 to AISI304. *Mater. Manuf. Process.* **34**(2), 192–200 (2018)
- Zhao, T.-S.; Zhou, J.; Zhou, J.-F.; Wu, D.-X.; Xiong, Y.: Influence of pre-stretching and aging processes on comprehensive performance of aluminum alloy. *Mater. Manuf. Process.* **33**(15), 1641–1647 (2018)
- de Miranda, A.C.O.; Gerlich, A.; Walbridge, S.: Aluminum friction stir welds: Review of fatigue parameter data and probabilistic fracture mechanics analysis. *Eng. Fract. Mech.* **147**, 243–260 (2015)
- Kayode, O.; Akinlabi, E.T.: An overview on joining of aluminium and magnesium alloys using friction stir welding (FSW) for automotive lightweight applications. *Mater. Res. Exp.* **6**(11), 112005 (2019). <https://doi.org/10.1088/2053-1591/ab3262>
- Ma, Z.Y.; Feng, A.H.; Chen, D.L.; Shen, J.: Recent advances in friction stir welding/processing of aluminum alloys: microstructural evolution and mechanical properties. *Crit. Rev. Solid State Mater. Sci.* **43**(4), 269–333 (2018)
- Jagesvar, V.; Taiwade, R.V.; Reddy, C.; Khatirkar, R.K.: Effect of Friction Stir Welding Process Parameters on Mg-AZ31B/Al-AA6061 Joints. *Mater. Manuf. Process* **33**, 308–314 (2017). <https://doi.org/10.1080/10426914.2017.1291957>
- Guoqiang, H.; Wu, J.; Hou, W.; Shen, Y.; Gao, J.: Producing of Al-WC surface composite by additive friction stir processing. *Mater. Manuf. Process* **34**, 147–158 (2018). <https://doi.org/10.1080/10426914.2018.1532590>
- Kumar Rajak, D.; Pagar, D.D.; Menezes, P.L.; Eyvazian, A.: Friction-based welding processes: friction welding and friction stir welding. *J. Adhes. Sci. Technol.* **34**(24), 2613–2637 (2020)
- Ghetiya, N.D.; Patel, K.M.; Kavara, A.J.: Multi-objective Optimization of FSW process parameters of aluminium alloy using taguchi-based grey relational analysis. *Trans. Indian Inst. Met.* **69**, 917–923 (2016)
- Chien, C.H.; Lin, W.B.; Chen, T.: Optimal FSW process parameters for aluminum alloys AA5083. *J. Chinese Inst. Eng.* **34**, 99–105 (2011)
- Costa, M.I.; Leitão, C.; Rodrigues, D.M.: Parametric study of friction stir welding induced distortion in thin aluminium alloy plates: a coupled numerical and experimental analysis. *Thin-Walled Struct.* (2019). <https://doi.org/10.1016/j.tws.2018.10.027>
- Zhang, G.; Zhao, H.; Xu, X.; Qiu, G.; Li, Y.; Lin, Z.: Metallic bump assisted resistance spot welding (MBaRSW) of AA6061-T6 and Bare DP590: Part II—joining mechanism and joint property. *J. Manuf. Process* (2019). <https://doi.org/10.1016/j.jmpro.2019.05.041>
- Shen, Z.; Ding, Y.; Gerlich, A.P.: Advances in friction stir spot welding. *Crit. Rev. Solid State Mater. Sci.* (2019). <https://doi.org/10.1080/10408436.2019.1671799>
- Krasnowski, K.; Hamilton, C.; Dymek, S.: Influence of the tool shape and weld configuration on microstructure and mechanical properties of the Al 6082 alloy FSW joints. *Arch. Civ. Mech. Eng.* **15**, 133–141 (2015)
- Cavaliere P.; Squillace A.; Panella F.: Effect of welding parameters on mechanical and microstructural properties of AA6082 joints produced by friction stir welding. *J. Mater. Process Technol.* **200**, 364–372 (2008)
- Sadeesh, P.; Venkatesh, K.M.; Rajkumar, V.; Avinash, P.; Arivazhagan, N.; Devendranath, R.K., et al.: Studies on friction stir welding of AA 2024 and AA 6061 dissimilar metals. *Procedia Eng.* **75**, 145–149 (2014)
- Momeni, M.; Guillot, M.: Post-weld heat treatment effects on mechanical properties and microstructure of AA6061-T6 butt joints made by friction stir welding at right angle (RAFSW). *J. Manuf. Mater. Process.* **3**(42), 1–13 (2019)
- Kwon, Y.J.; Shim, S.B.; Park, D.H.: Friction stir welding of 5052 aluminum alloy plates. *Trans. Nonferr. Met. Soc. China* **19**, 23–27 (2009)
- Moshwan, R.; Yusof, F.; Hassan, M.A.; Rahmat, S.M.: Effect of tool rotational speed on force generation, microstructure and mechanical properties of friction stir welded Al-Mg-Cr-Mn (AA 5052-O) alloy. *Mater. Des.* **66**, 118–128 (2015)
- Mustafa, F.F.; Kadhym, A.H.; Yahya, H.H.: Tool geometries optimization for friction stir welding of AA6061-T6 aluminum alloy T-joint using taguchi method to improve the mechanical behavior. *J. Manuf. Sci. Eng. Trans. ASME* **137**, 1–8 (2015)
- Hong, S.T.; Kwon, Y.J.; Son, H.J.: The mechanical properties of friction stir welding (FSW) joints of dissimilar aluminum alloys. In: 1st International Symposium on Hybrid Materials and Processing, Busan, South Korea, Paper 69 (2008)
- Park, S.K.; Hong, S.T.; Park, J.H.; Park, K.Y.; Kwon, Y.J.; Son, H.J.: Effect of material locations on properties of friction stir welding joints of dissimilar aluminum alloys. *Sci. Technol. Weld Join.* **15**(4), 331–336 (2010)
- Howeyze, M.; Arabi, H.; Eivani, A.R.; Jafarian, H.R.: Strengthening of AA5052 aluminum alloy by equal channel angular pressing followed by softening at room temperature. *Mater. Sci. Eng. A* **720**, 160–168 (2018)
- Ilangovan, M.; Rajendra Boopathy, S.; Balasubramanian, V.: Effect of tool pin profile on microstructure and tensile properties of friction stir welded dissimilar AA 6061-AA 5086 aluminium alloy joints. *Def. Technol.* **11**(2), 174–184 (2015)
- Shanmuga Sundaram, N.; Murugan, N.: Tensile behavior of dissimilar friction stir welded joints of aluminium alloys. *Mater. Des.* **31**, 4184–4193 (2010)
- Lakshminarayanan, A.K.; Balasubramanian, V.: Process parameters optimization for friction stir welding of RDE-40 aluminium alloy using Taguchi technique. *Trans. Nonferr. Met. Soc. China* **18**(3), 548–554 (2008)
- Vignesh, K.; Elaya Perumal, A.; Velmurugan, P.: Optimization of resistance spot welding process parameters and microstructural examination for dissimilar welding of AISI 316L austenitic stainless steel and 2205 duplex stainless steel. *Int. J. Adv. Manuf. Technol.* **93**(1), 455–465 (2017)



30. Thirumavalavan, K.; Chandrasekhar, S.C.M.A.; Muruganandhan, R.; Muthu Manickam, M.A.: Study on the influence of process parameters of severe surface mechanical treatment process on the surface properties of AA7075 T651 using TOPSIS and Taguchi analysis. *Mater. Res. Exp.* **6**, 11 (2019)
31. Abdelhady, S.S.; Zoalfakar, S.H.; Agwa, M.A.; Ali, A.A.: Electrospinning process optimization for Nylon 6,6/Epoxy hybrid nanofibers by using Taguchi method. *Mater. Res. Exp.* **6**, 95314 (2019)
32. Kumar, S.; Singh, R.: Optimization of process parameters of metal inert gas welding with preheating on AISI 1018 mild steel using grey based Taguchi method. *Measurement* **148**(3), 1–12 (2019)
33. Xavior, A.; Adithan, M.: Determining the influence of cutting fluids on tool wear and surface roughness during turning of AISI 304 austenitic stainless steel. *J. Mater. Process Technol.* **209**(2), 900–909 (2009)
34. Heidarzadeh, A.; Saeid, T.; Klemm, V.: Microstructure, texture, and mechanical properties of friction stir welded commercial brass alloy. *Mater. Charact.* **119**, 84–91 (2016)
35. Heidarzadeh, A.; Pouraliakbar, H.; Mahdavi, S.; Jandaghi, M.R.: Ceramic nanoparticles addition in pure copper plate: FSP approach, microstructure evolution and texture study using EBSD. *Ceram Int.* **44**(3), 3128–3133 (2018)
36. Sato, Y.S.; Urata, M.; Kokawa, H.: Parameters controlling microstructure and hardness during friction-stir welding of precipitation-hardenable aluminum alloy 6063. *Metall. Mater. Trans. A* **33**, 625–635 (2002)
37. El-Hafez, H.A.: Mechanical properties and welding power of friction stirred AA2024-T35 joints. *J Mater Eng Perform.* **20**(6), 839–845 (2011)
38. Bagheri, B.; Abbasi, M.; Dadaei, M.: Mechanical behavior and microstructure of AA6061-T6 joints made by friction stir vibration welding. *J. Mater. Eng. Perform.* (2020). <https://doi.org/10.1007/s11665-020-04639-7>
39. Sharma, N.; Siddiquee, A.N.; Khan, Z.A.; Mohammed, M.T.: Material stirring during FSW of Al-Cu: effect of pin profile. *Mater. Manuf. Process.* **33**(7), 786–794 (2018)
40. Vijayavel, P.; Balasubramanian, V.: Effect of pin volume ratio on wear behaviour of friction stir processed LM25AA-5%SiCp metal matrix composites. *Alexandria Eng J.* **57**, 2939–2950 (2018)
41. Elangovan, K.; Balasubramanian, V.: Influences of tool pin profile and tool shoulder diameter on the formation of friction stir processing zone in AA6061 aluminium alloy. *Mater. Des.* **29**, 362–373 (2008)
42. Marzbanrad, J.; Akbari, M.; Asadi, P.; Safaee, S.: Characterization of the influence of tool pin profile on microstructural and mechanical properties of friction stir welding. *Metall. Mater. Trans. B* **45**, 1887–1894 (2014)
43. McNelley, T.R.; Swaminathan, S.; Su, J.Q.: Recrystallization mechanisms during friction stir welding/processing of aluminum alloys. *Scr. Mater.* **58**, 349–354 (2008)
44. Ahmadnia, M.; Shahraki, S.; Kamarposhti, M.A.: Experimental studies on optimized mechanical properties while dissimilar joining AA6061 and AA5010 in a friction stir welding process. *Int. J. Adv. Manuf. Technol.* **87**, 5–8 (2016)

